Mon. Not. R. astr. Soc. (1968) **138,** 181–212.

THE ABUNDANCES OF THE ELEMENTS IN THE SOLAR PHOTOSPHERE—II

Sodium, Aluminium, Phosphorous, Sulphur and Potassium

D. L. Lambert and B. Warner†*

(Received 1967 July 27)

Summary

A comprehensive account is given of the available solar absorption lines arising from the elements sodium, aluminium, phosphorus, sulphur and potassium. The use of improved oscillator strengths for selected lines leads to a revision of the abundances of these elements. The final values, on the scale log $N(\mathrm{H}) = 12{\cdot}00$, are

$$\log N(\mathrm{Na}) = 6{\cdot}18$$
$$\log N(\mathrm{Al}) = 6{\cdot}40$$
$$\log N(\mathrm{P}) = 5{\cdot}43$$
$$\log N(\mathrm{S}) = 7{\cdot}21$$
$$\log N(\mathrm{K}) = 5{\cdot}05.$$

1.1 *Introduction.* In the first paper of this series (Lambert 1967a) it was pointed out that there is a need for a complete revision of solar abundances, making use of the availability of more accurate data on equivalent widths, oscillator strengths and the solar model. This study is continued by a discussion of all available lines of a number of atoms for which reliable oscillator strengths can be readily calculated.

The abundances of the alkalis sodium and potassium are of special interest as in very cool stars they may become the dominant contributors of electrons. Vardya (1966) has pointed out that an accurate value of the solar sulphur abundance would help to decide the importance of HS^- and S^- absorption in M dwarf stars. A recent discussion of neutral phosphorus lines in the solar spectrum (Swensson 1966) has resulted in a number of new identifications and these should lead to an improvement in the abundance determination. Finally, aluminium is a minor electron donor in the solar atmosphere but becomes relatively more important in the cooler stars.

The method of extracting abundance data from measurements of equivalent widths is well known and was summarized in Paper I. In general, for the present study greatest weight is given to lines with wavelengths greater than 6000 Å. In this wavelength region the known continuous absorption coefficients satisfactorily account for the observed continuum, line blending is usually minimal so that accurate equivalent widths may be measured, and the calculated oscillator strengths usually refer to transitions between excited states and are accordingly more reliable.

1.2 *Sources of equivalent widths.* The three principal sources of equivalent widths were noted in Paper I. They are:

The Table of Solar Spectrum Wavelengths, 11 984–25 578 Å, Mohler (1955).

The Preliminary Photometric Catalogue of Fraunhofer Lines, λ 3164–λ 8770, Utrecht (1960), and

* Present address: Mount Wilson and Palomar Observatories, Pasadena, California.
† Present address: Department of Astronomy, University of Texas, Austin, Texas.

The Photometric Atlas of the Solar Spectrum, λ 7498–λ 12 016, Delbouille & Roland (1963).

Additional sources were consulted and full details are given in the line lists for each element.

A careful comparison was made of the equivalent widths given in the Preliminary Photometric Catalogue (PPC) with the present measurements made from the tracings of the Delbouille & Roland Atlas. Especial emphasis was given to a comparison of weak lines ($W_\lambda \leqslant 10$ mÅ). For the stronger lines the two sources show no systematic difference. In the interval λ 8000 ± 200 Å lines with equivalent widths of 2, 3, 5 and 7 mÅ according to the PPC were measured on the Delbouille and Roland Atlas. In the selection of lines, telluric lines and blends of telluric and solar lines were excluded. For this purpose the recently published revision of Roland's Table of Solar Wavelengths was consulted (Moore, Minnaert & Houtgast 1966, referred to below as RRT). The results of the comparison are summarized in Table I. The measurements off the Delbouille and Roland Atlas appear to yield systematically smaller equivalent widths. However, the difference in each case is less than two standard deviations. It is concluded that these two sources provide similar equivalent widths for the weak lines.

TABLE I

A comparison of equivalent widths given in the Preliminary Photometric Catalogue with those obtained by measurement off the Delbouille & Roland Atlas. Wavelength interval 8000 ± 200 *Å* W_λ *in mÅ*

W_λ (PPC)	W_λ (D–R)	No. of lines
2	1·8 ± 0·2	10
3	2·5 ± 0·3	10
5	4·6 ± 0·4	10
7	6·7 ± 0·4	10

1.3 *Oscillator strengths.* The central problem in the determination of reliable abundances in the atmospheres of the Sun and stars is the need for accurate oscillator strengths for the observed transitions. For the elements of light and medium atomic weight, the available experimental data is often fragmentary and may refer entirely to lines in the ultraviolet which are excluded from the present study. Therefore, calculated oscillator strengths must be used.

By applying the standard techniques of atomic physics it is possible to calculate oscillator strengths of high accuracy for many lines in the spectra of the lighter elements. In later papers in this series, oscillator strengths calculated on the theory of intermediate coupling with configuration mixing will be used to provide improved abundance determinations. However, in some atoms it is evident that the effects of departures from LS coupling and of configuration interaction are small, at least for the transitions of astrophysical interest. The atoms studied in this paper fall in this latter category. Eventually, of course, the more sophisticated theory will be applied but it is expected that it will justify the present circumvention of most of the detailed calculation.

The calculation of the oscillator strengths reduces to the following three items:

(i) the calculation of the relative line strengths,
(ii) the calculation of the radial integral, and
(iii) the delineation of regions of applicability of the simple theory.

Throughout this paper LS coupling line strengths are adopted, but it should be pointed out that for other transitions in the considered atoms it might be more appropriate to adopt a different coupling scheme (e.g. *jJ* or *jK* coupling for transitions between highly excited states).

The radial integrals are calculated from wavefunctions, which may be computed by several methods. The wavefunctions obtained from a semi-empirical method (e.g. the Coulomb approximation of Bates & Damgaard (1949), or the improvements due to Stewart & Rotenberg (1965) and Warner (1967) and known as the STF method), which uses an experimental energy as the eigenvalue in the one-electron Schrödinger equation, are expected to be superior to those given by the Hartree–Fock method (which neglects correlation). The former are adopted here.

Finally, the transitions for which these calculations are expected to be valid are to be determined *ad hominem*. Indications of their validity are obtained through a comparison of energy intervals within terms and available Lande *g*-factors with the predictions of LS coupling. The term tables may also be inspected for possible interacting configurations. Furthermore, inspection of a detailed laboratory line list will indicate those levels which give rise to intercombination lines (an indication of spin–orbit interaction) or interparental transitions (due primarily to configuration mixing). As a final resort, one may choose to determine the abundance only from those multiplets having LS coupling relative line intensities. Full details of the application of these ideas are given in the discussion of individual elements.

1.4 *Damping constants*. The necessary damping parameters were evaluated by standard techniques (see e.g. Aller 1963). Three components of the damping constant were considered: van der Waals broadening, Stark broadening and radiative damping. The van der Waals constants were found from Coulomb wavefunctions. Stark broadening coefficients were taken from the tabulations of Griem (1964) or were calculated from Hunger's (1960) method. Finally, the radiative damping constants were determined by summing over all downward transitions from the upper and lower level for the desired line.

2. *Sodium*

2.1 *Introduction*. In Table II details are given for 31 Na I lines present in the solar spectrum. This selection is based upon the compilation given by Risberg (1956). The Na I lines identified in the RRT are listed in Table II except for eight weak lines between λ4000 and λ5000 Å.

The previous studies of Na I lines in the solar spectrum (Goldberg, Müller & Aller 1960, referred to below as GMA, Mugglestone & O'Mara 1966) were concerned almost exclusively with the $3p$–ns and $3p$–nd transitions. Here, the discussion is broadened to include certain $3d$–nf, $4s$–np, and $4p$–nd transitions.

2.2 *Oscillator strengths*. Apart from absorption measurements on the principal series, there are very few experimental measurements of oscillator strengths in Na I. Most of the laboratory measurements were discussed by GMA, who concluded that, for the transitions used by them, there is good agreement with the Coulomb approximation calculations.

For the present study, the oscillator strengths were calculated from Coulomb approximation wave functions with allowance for configuration mixing in the *nl*

Table II

Na I *lines in the solar spectrum*

Transition array	Multiplet	Δj	$\lambda_\odot$	χ	log gf	W_λ L	W_λ RRT	W_λ M	log $W_\lambda/\lambda+7$	Notes
$3s$–$3p$	^2S–$^2P^0$	1/2–3/2	5889·973	0·00	+0·11		633	765★		
		1/2–1/2	5895·940		−0·19		557	570★		
$3s$–$4p$	^2S–$^2P^0$	1/2–3/2	3302·283	0·00	−1·17		112		2·53	
		1/2–1/2	3302·982		−2·01		83		2·40	
$3p$–$4s$	$^2P^0$–^2S	3/2–1/2	11403·80	2·10	−0·19	240:			2·32	(1)
		1/2–1/2	11381·45		−0·49	178:			2·19	(1)
$3p$–$5s$	$^2P^0$–^2S	3/2–1/2	6160·753	2·10	−1·27		44	53★	1·90	
		1/2–1/2	6154·230		−1·57		27	36★	1·70	
$3p$–$6s$	$^2P^0$–^2S	3/2–1/2	5153·410	2·10	−1·77		24:		1·67	(2)
		1/2–1/2	5148·846		−2·07		14		1·44	
$3p$–$7s$	$^2P^0$–^2S	3/2–1/2	4751·825	2·10	−2·10		15	13★	1·47	
		1/2–1/2	4747·96		−2·40			6:	1·10	(2)
$3p$–$3d$	$^2P^0$–^2D	3/2–3/2, 5/2	8194·836	2·10	+0·53	315	304		2·57	(3)
		1/2–3/2	8183·25		+0·22	236	180		2·46	(4)
$3p$–$4d$	$^2P^0$–^2D	3/2–3/2, 5/2	5688·217	2·10	−0·40		121	128★	2·35	
		1/2–1/2	5682·647		−0·71		104		2·26	
$3p$–$5d$	$^2P^0$–^2D	3/2–3/2, 5/2	4982·825	2·10	−0·91		83		2·23	
		1/2–3/2	4978·555		−1·22		38:		1·88	(2)
$3p$–$6d$	$^2P^0$–^2D	3/2–3/2, 5/2	4668·572	2·10	−1·25		39		1·92	

$3p$–$7d$	$^2P^0$–^2D	3/2–3/2, 5/2	4497·680	2·10	−1·52		27	1·78	
		1/2–3/2	4494·196		−1·82		18:	1·60	(2)
$3d$–$5f$	^2D–$^2F^0$		12679·24	3·62	+0·20		83†:	1·82	(1)
$3d$–$6f$	^2D–$^2F^0$		10834·85	3·62	−0·25		33	1·50	
$3d$–$7f$	^2D–$^2F^0$		9961·38	3·62	−0·58		15	1·18	
$3d$–$8f$	^2D–$^2F^0$		9465·98	3·62	−0·82		7:	0·87	(1)
$4s$–$4p$	^2S–$^2P^0$	1/2–3/2	22056·62	3·19	+0·28		300†	2·13	
		1/2–1/2	22083·93		−0·02		276†		(5)
$4s$–$5p$	^2S–$^2P^0$	1/2–3/2	10746·44	3·19	−1·30	13		1·08	(6)
$4p$–$4d$	$^2P^0$–^2D	3/2–3/2, 5/2	23379·28	3·75	+0·58		240†:	2·01	(1)
		1/2–3/2	23348·82		+0·28		237†:	2·00	(7)
$4p$–$5d$	$^2P^0$–^2D	3/2–3/2, 5/2	14779·89	3·75	−0·29		36†:	1·39	(8)

Notes to Table II:

(1) Na line in wing of strong telluric line: W_λ uncertain.
(2) Inspection of the Utrecht Atlas shows this line to be seriously blended.
(3) Allen (1936) and Righini (1935) give $W_\lambda = 253$ and 263 respectively.
(4) Measurement of the Utrecht Atlas gives $W_\lambda = 265$ mÅ. Righini (1935) gives $W_\lambda = 195$. The Liege Atlas measurement is adopted.
(5) Blended with a Si I line.
(6) This line may be a blend of Na I and a telluric line.
(7) Mohler (1955) lists a telluric CO line as a contributor to this line. According to neighbouring CO lines $W_\lambda \simeq 10$ mÅ for the CO line.
(8) Blend with C I $3p^3P_0$–$4s^3P_1^0$ for which the predicted $W_\lambda \simeq 8$ mÅ.

★ W_λ from McMath–Hulbert tracings (Holweger 1967).
† W_λ from Mohler (1955).

levels due to spin–orbit interaction (Warner 1967). This latter interaction has an almost negligible effect in Na I. Indeed, this conclusion can be anticipated from the small doublet splitting in the *np* terms. The calculations of the transition integrals were examined and no examples of strong cancellation of the positive and negative contributions were found.

The calculated oscillator strengths are in very close agreement with those given by Anderson & Zilitis (1964) who used a modified Coulomb approximation.

The oscillator strength for the Na I *D* lines is obtained from accurate lifetime measurements (Stephenson 1951, Demtroder 1962, Hulpke *et al.* 1964, Karstenson 1965). The total oscillator strength for the $3s$–$3p$ transition ($gf = 1{\cdot}96 \pm 0{\cdot}01$) agrees well with that given by the Coulomb approximation (1·87), the STF method (1·95), and the method of Anderson & Zilitis (1·94).

2.3 Curves of growth were calculated for individual multiplets. Radiative, Stark, and van der Waals damping were taken fully into account. Mugglestone & O'Mara (1966) stressed the importance of Stark damping for certain transitions (notably λ 5682, 5688 and 4982 Å).

The abundance determinations for individual lines are summarized in Table III. The apparently wide range in the abundances led to the adoption of a simple system of weights which are based upon the quality of the equivalent width measurement. Weight zero is given to heavily blended lines or to lines for which an identified blend is listed in Table II. Weight four is given to lines which are free from blends. The weighted mean abundance is

$$\log \frac{N_{\mathrm{Na}}}{N_{\mathrm{H}}} = -5{\cdot}82 = 6{\cdot}18 - 12{\cdot}00.$$

The Na *D* lines and the transition $3s$–$5p$, which are not considered for the mean abundance, are discussed below. The unweighted mean, which included all lines in Table III, is within 0·01 dex of the above abundance. It is shown below that the wings of the Na *D* lines indicate that the theoretical damping constants underestimate the true damping by almost a factor two. In view of this, the abundance determinations from the strong lines should be considered uncertain. However, a further average over the weaker lines, which are insensitive to an incorrect choice of damping constant, provides an abundance only 0·01 smaller than the weighted mean for all lines.

The wide range in the results given in Table III is a little surprising. Na I is a one-electron spectrum and one would expect the theoretical oscillator strengths to be reliable. Two possible explanations may be proposed. First, for the strong lines the damping constants may have been underestimated with a resultant overestimate for the abundance. Table III contains a certain amount of evidence to support this claim. Second, a number of the weaker lines might be seriously blended with unidentified lines. It is especially noticeable that the weak lines from the $3p$–ns series give a markedly higher abundance than similar lines from the $3p$–nd, and $3d$–nf series. Examination of the lines in the $3p$–ns series revealed that in all except two cases the equivalent width must be assumed uncertain. It is conjectured that for the two relatively unblended lines λ 5148 and λ 4751, which give [Na]* = +0·05 and +0·11 respectively, the identification Na I might be incomplete. Unfortunately, a search for alternative identifications was unsuccessful.

* $[X] = \log N(X) - \log N_{\mathrm{GMA}}(X)$.

TABLE III

Sodium abundance results for individual lines

Transition array	λ	[Na]*	Weight	Transition array	λ	[Na]	Weight
$3p$–$4s$	11403	0·00	2	$3d$–$5f$	12679	−0·42	1
	11381	−0·12	1				
				$3d$–$6f$	10834	−0·23	4
$3p$–$5s$	6160	−0·11	4				
	6154	−0·09	4	$3d$–$7f$	9961	−0·21	4
$3p$–$6s$	5153	+0·02	0	$3d$–$8f$	9465	−0·28	1
	5148	+0·05	3				
				$4s$–$4p$	22056	−0·20	2
$3p$–$7s$	4751	+0·11	2		22083	+0·06	0
	4747	0·00	0				
				$4s$–$5p$	10746	−0·04	2
$3p$–$3d$	8194	+0·04	2				
	8183	−0·07	2	$4p$–$4d$	23378	−0·29	1
					23348	0·00	1
$3p$–$4d$	5688	−0·21	2				
	5682	−0·11	1	$4p$–$5d$	14779	−0·14	0
$3p$–$5d$	4982	−0·13	2				
	4978	−0·30	0				
$3p$–$6d$	4668	−0·26	3				
$3p$–$7d$	4497	−0·16	3				
	4494	−0·05	0				

* [Na] = $\log N(\mathrm{Na}) - \log N_{\mathrm{GMA}}(\mathrm{Na})$.

If it is assumed that the theoretical oscillator strengths are reliable, the positive abundance corrections [Na] for some $3p$–ns lines can be explained as the result of blending with unidentified lines. The mean abundance from the weaker lines in only the $3p$–nd and $3d$–nf series is [Na] = −0·22, or 0·10 dex smaller than the weighted mean for all lines. In the absence of a positive identification for the suggested blended features, one must accept the weighted mean abundance but it should be noted that this might be an overestimate by about 0·10 dex.

The weighted mean abundance, which is smaller than the GMA value on account of their omission of the line broadening factors, is very close to the value obtained by Mugglestone & O'Mara ($\log N_{\mathrm{Na}} = -5{\cdot}85$).

2.4 *Discussion.* The Na *D* lines were not included in the discussion of the abundance. The assumption of local thermodynamic equilibrium (LTE) which is adopted in the present calculations, is expected to be invalid for the region responsible for the formation of the *D* line cores. Nonetheless, the assumption of LTE should be applicable to an interpretation of the wings of the *D* lines. In the wing, the line depth is proportional to the product of the damping constant and the

abundance. A good fit to the observed profiles (Waddell 1962) can be obtained with the revised abundance and the experimental oscillator strength, but only through an increase of the damping constant by a factor 1·8 above the theoretical value. A similar result was obtained by Chamaraux (1967). As an alternative, the adoption of the theoretical damping constant results in an abundance which is 0·25 dex larger than the revised value. No other lines give such a large abundance. This discrepancy suggests that accurate line profile observations for other strong Na I lines would be of the greatest interest.

Since the sources of continuous opacity at λ 3302 are not well known, the $3p$–$4s$ transition was omitted from the abundance determination. A curve of growth was calculated on the assumption that the H^- ion and the neutral H atom were the only opacity sources. The derived abundances are

$$\lambda\,3302{\cdot}2 \qquad [\mathrm{Na}] = -0{\cdot}15$$
$$\lambda\,3302{\cdot}9 \qquad = -0{\cdot}41$$

compared with the average abundance correction [Na] = −0·12. The discrepancy would be reduced if the additional opacity, which is necessary to explain the continuous spectrum, were introduced.

The partial list of Na I lines in the solar spectrum, which was given in Table II, is extended in Table IV. This table gives the predicted and observed equivalent widths for a number of weak lines and for recognized belends. Several new identifications are proposed.

With the exception of the Na *D* lines, the important information, which may be extracted from line profile observations, has not been considered in this discussion. It would be of great value to obtain accurate line profiles for certain Na I

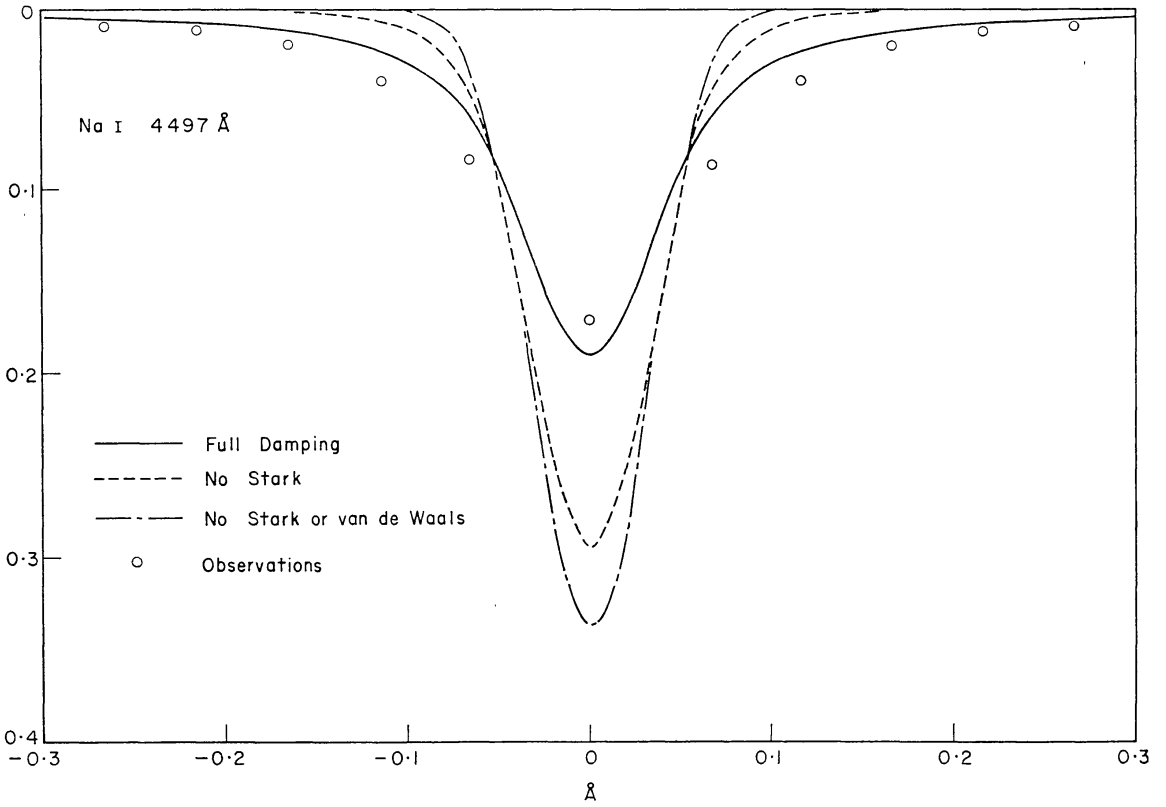

FIG. 1. *Observed and calculated profiles of Na* I 4497 *Å.*

TABLE IV

Suggested identifications of Na I lines in the solar spectrum

Multiplet	Δj	λ	$\lambda_\odot$	W_λ Predicted	W_λ Observed	Identification	Notes
$3p^2P^0$–$8s^2S$	3/2–1/2	4545·186	1·61	4·7			(2)
	1/2–1/2	4541·633		2·3		Na I	(1)
$3p^2P^0$–$9s^2S$	3/2–1/2	4423·246	3·265	2·8	37	Na I, Cr I	
	1/2–1/2	4419·885		1·4			(2)
$3p^2P^0$–$10s^2S$	3/2–1/2	4344·746	4·746	1·2	3·5	Na I	
	1/2–1/2	4341·489		0·6			(2)
$3p^2P^0$–$6d^2D$	1/2–3/2	4664·811	4·794	28	52	Cr I, Na I	
$3p^2P^0$–$8d^2D$	3/2–5/2, 3/2	4393·340	3·33	17		Na I	(1)
	1/2–3/2	4390·029		8			(2)
$3p^2P^0$–$9d^2D$	3/2–5/2, 3/2	4324·616	4·616	11	6	Na I	
	1/2–3/2	4321·401	1·412	5·3	9·5	Na I	
$3p^2P^0$–$10d^2D$	3/2–5/2, 3/2	4276·787	6·826	7·8	7	Na I?	
	1/2–3/2	4273·643		3·7			(2)
$3p^2P^0$–$11d^2D$	3/2–5/2, 3/2	4242·081		5·5			(2)
	1/2–3/2	4238·988		2·7			(2)
$3d^2D$–$4f^2F^0$		18465·25		300			(2)
$3d^2D$–$9f^2F^0$		9153·878	3·82	6	4	Na I, CN	(3)
$3d^2D$–$10f^2F^0$		8942·962	2·95	4	4:	Na I	(4)
$4s^2S$–$6p^2P^0$	1/2–1/2	8650·889	0·91	0·8	2:	Atm? Na I	(4)
	1/2–3/2	8649·922	9·95	1·7	2·5:	Na I	(4)
$4s^2S$–$7p^2P^0$	1/2–3/2	7809·781		0·6		Absent	(5)
$4p^2P^0$–$6s^2S$	3/2–1/2	16388·85	8·93	16	27	Na I, CO_2	(6)
	1/2–1/2	16373·85		8		CH_4	(2)
$4p^2P^0$–$7s^2S$	3/2–1/2	12917·26		2·6		Absent	
	1/2–1/2	12907·94		1·3		Absent	
$4p^2P^0$–$6d^2D$	3/2–3/2, 5/2	12319·98	0·28	17	28	Na I?	(4)
	1/2–3/2	12311·48	1·49	9	20	Na I? HOH	(4)
$4p^2P^0$–$7d^2D$	3/2–3/2, 5/2	11197·21		7			(2)
	1/2–3/2	11190·19		4			(2)

Notes to Table IV:

(1) Observed in sunspot only according to RRT.

(2) Masked by stronger solar or telluric line.

(3) New identification. Babcock & Moore (1947) suggest λ 9154·122 might be Na I. The CN line is (1, 0) $Q_2(4)$ with a predicted W_λ = 2 mÅ.

(4) New Identification.

(5) $W_\lambda \leq 1$ mÅ.

(6) Mohler (1955) predicts for the CO_2 line W_λ = 13 mÅ.

lines. For example, Mugglestone & O'Mara pointed out that Stark broadening is the dominant contributor to the damping constant for certain transitions. λ 4497 is one such case. Since this is a weak line, the derived abundance is insensitive to

1968MNRAS.138..181L

TABLE V

Al I *lines in the solar spectrum*

Transition array	Multiplet	Δj	$\lambda_\odot$	χ	log gf	L	W_λ RRT	M	log $W_\lambda/\lambda+7$	Notes
$3p$–$4s$	$^2P^0$–^2S	3/2–1/2	3961·535	0·00	−0·32		621		3·20	
		1/2–1/2	3944·016		−0·62		488		3·09	
$4s$–$4p$	^2S–$^2P^0$	1/2–3/2	13123·32	3·14	+0·20			366†	2·45	(1)
		1/2–1/2	13150·76		−0·09			359†:	2·29	
$4s$–$5p$	^2S–$^2P^0$	1/2–3/2	6696·032	3·14	−1·33*		33		1·69	
		1/2–1/2	6698·669		−1·63*		21		1·50	
$4s$–$6p$	^2S–$^2P^0$	1/2–3/2	5557·070	3·14	−1·96*		5	5	0·95	
$3d$–$5p$	^2D–$^2P^0$	3/2–1/2	12757·45	4·02	−2·07*			4†	0·50	
$3d$–$5f$	^2D–$^2F^0$	5/2–7/2, 5/2	8773·906	4·02	−0·07	108		99	2·07	
		3/2–5/2	8772·884		−0·25	77		80	1·95	
$3d$–$6f$	^2D–$^2F^0$	5/2–7/2, 5/2	7836·130	4·02	−0·40	65	64		1·92	
		3/2–5/2	7835·317		−0·58	43	42		1·74	
$3d$–$7f$	^2D–$^2F^0$	5/2–7/2, 5/2	7361·291	4·02	−0·65		43		1·77	
		3/2–5/2	7361·550		−0·83		31		1·62	(2)
$3d$–$8f$	^2D–$^2F^0$	5/2–7/2, 5/2	7084·656	4·02	−0·86		17		1·38	

4*p*–5*s*	$^2P^0$–^2S	3/2–1/2	21163·88	4·09	−0·03		372†	2·25
		1/2–1/2	21093·19		−0·33		280†	2·12
4*p*–6*s*	$^2P^0$–^2S	3/2–1/2	10891·74	4·09	−1·10	30		1·44
		1/2–1/2	10872·98		−1·40	14		1·11
4*p*–7*s*	$^2P^0$–^2S	3/2–1/2	8841·23	4·09	−1·59	6·4		0·86
		1/2–1/2	8828·87		−1·89	3·2		0·56
4*p*–4*d*	$^2P^0$–^2D	3/2–5/2	16750·65	4·09	+0·54		467†	2·45
		1/2–3/2	16719·12		+0·28		370†	2·34
		3/2–3/2	16763·36		−0·42		158†	1·94
4*p*–5*d*	$^2P^0$–^2D	3/2–5/2	10781·97	4·09	−1·26*	9·6		0·95
		1/2–3/2	10768·35		−1·52*	4·9		0·66
4*p*–6*d*	$^2P^0$–^2D	1/2–3/2	8912·94	4·09	−2·36*	2·3		0·41 (3)
5*s*–6*p*	^2S–$^2P^0$	1/2–3/2	17699·38	4·67	−1·17		13†	0·87

Notes to Table V:

(1) According to Mohler (1955) Zn I may be a contributor to this line.
(2) RRT suggests that a Ti I line may be a contributor.
(3) Possibly a blend: see text.

* Uncertain value owing to cancellation effects.
† W_λ From Mohler (1955).

the assumed damping constant. However, the line profile reveals the effects of the Stark broadening. This is illustrated in Fig. 1. where the profile of the line in the Utrecht Atlas (and uncorrected for the instrumental profile) is compared with computed profiles, which are normalized to give the observed equivalent width. The observed wings are very broad and can be reproduced when the Stark broadening is included in the calculations. For other lines van der Waals broadening is dominant and for transitions such as $3d$–$7f$, $8f$ results in large damping constants. Again, the effect on the line profile is apparent even on existing tracings: $3d$–$7f$ λ 9961 is a weak line which appears on the Liège Atlas with a very broad, almost pure dispersion, profile.

3. *Aluminium*

3.1 *Introduction.* The laboratory spectrum of Al I was discussed recently by Eriksson & Isberg (1963) who also listed possible identifications for Al I lines in the solar spectrum. A total of 28 lines were selected with good equivalent width determinations and details are given in Table V. A line at λ 3900·660 is identified in the RRT as Al II? This identification is discussed below.

3.2 *Oscillator strengths.* The only reliable experimental oscillator strengths in Al I are lifetime measurements for the resonance lines $3p^2P$–$4s^2S$ (Demtroder 1962). These are quoted in Table V.

For all other transitions, calculated oscillator strengths are adopted. The two important features of the observed transitions are the unreliability of some radial integrals because of cancellation effects, and the non-Coulombic nature of the $3d$ state. The transitions for which strong cancellation occurs are $3d$–$5p$, $4p$–$5d$, $4p$–$6d$, $4s$–$6p$ and to a less extent $4s$–$5p$.

The $3d$–nf transitions provide 7 lines, and much weight was given to these by GMA, who used Coulomb approximation calculations for the oscillator strengths. However, since the effective quantum number for $3d$ is 2·63, the coulomb approximation is inapplicable. In addition, Froese (1967) finds that $3s^23d$ is only 91 per cent pure. If allowance is made for both of these effects, the oscillator strengths are 0·12 dex smaller than the Coulomb approximation values. A smaller correction of $-0{\cdot}04$ dex is applied to the values involving the $3s^24d$ state.

Interparental transitions of the type $3s^2(^1S)nd$–$3s3p(^3P)n'd$ are observed. It is presumed that these result from mixing of the upper terms with $3s^2np$ or other configurations.

3.3 *Abundance.* The abundance determinations, which are presented in Table VI, were obtained from curves of growth calculated for the individual multiplets. The weights were assigned according to the degree of blending of the Al I lines. The transitions for which the radial integral is unreliable owing to cancellation effects are not given in Table VI. The resonance lines ($3p$–$4s$) are discussed separately.

The weighted mean abundance for the 18 lines in Table V is 0·20 dex larger than the GMA abundance, that is

$$\log \frac{N_{\mathrm{Al}}}{N_{\mathrm{H}}} = -5{\cdot}60 = 6{\cdot}40 - 12{\cdot}00.$$

A closer analysis of the results is of interest. The series $4p$–ns gives a mean abundance [Al] = +0·31, or +0·25 if the two strong lines at 2·1 microns are

omitted. The seven lines belonging to the series $3d$–nf give [Al] = +0·13, which is significantly smaller than the value based on the $4p$–ns series. This discrepancy is increased by 0·11 dex if the Coulomb approximation radial integrals and LS line strengths are adopted for the $3d$–nf series. The present discrepancy of 0·12 to 0·18 dex suggests that a more thorough treatment of the $3d$ state is desirable. However, the correction to the above mean abundance is unlikely to exceed +0·10 and is probably less than +0·05 dex.

The transitions which were rejected because of cancellation effects give a mean abundance 0·24 dex smaller than the present value. This discrepancy illustrates the necessity to identify and reject such transitions when determining an abundance. The line λ 8912 ($4p$–$6d$) was not considered because it gives [Al] = +0·55 which suggests that the Fraunhofer line is not wholly attributable to Al I.

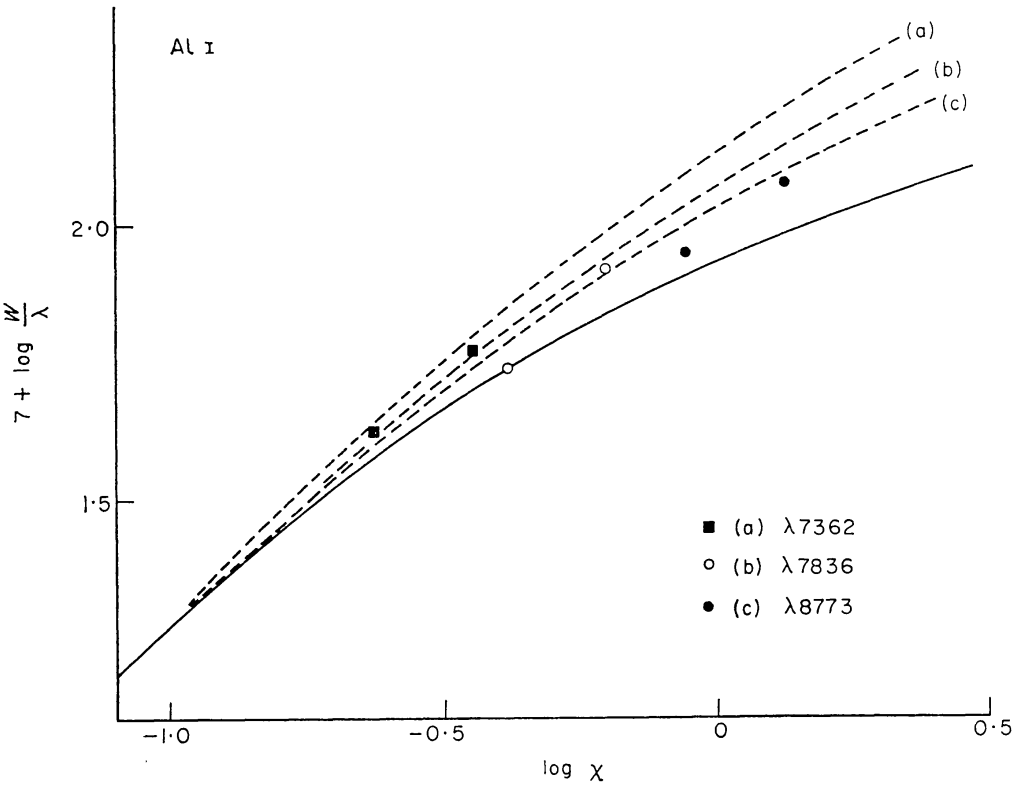

FIG. 2. *Curves of growth for Al* I $3d$–nf *transitions. The solid line is the theoretical curve for zero damping* (8773 Å).

The importance of calculating the damping constants for each multiplet is illustrated by Fig. 2. This gives curves of growth with the appropriate damping constants for $3d$–$5f$, $6f$ and $7f$. A curve of growth for zero damping is also shown. The differences in the shapes of the curves of growth are chiefly attributable to an increase in the van der Waals broadening.

3.4 *Discussion.* The Al I resonance lines at λ 3961 and 3944 fall in the wings of the strong Ca II H and K lines, and without a detailed treatment, must be supposed unsuitable for an abundance determination. The straightforward application of the curve of growth method, which omits the effects of both the Ca II H and K line absorption and the unidentified opacity sources known to be present from studies of the continuous spectrum, gives a mean abundance for these two

TABLE VI

Aluminium abundance results for individual lines

Transition	λ	[Al]	Weight
$4s$–$4p$	13123	+0·26	2
	13150	+0·05	1
$3d$–$5f$	8773	+0·16	3
	8772	+0·12	2
$3d$–$6f$	7836	+0·16	4
	7835	+0·11	3
$3d$–$7f$	7362	+0·17	3
	7361	+0·17	2
$3d$–$8f$	7084	−0·05	2
$4p$–$5s$	21163	+0·48	2
	21093	+0·49	2
$4p$–$6s$	10891	+0·32	3
	10872	+0·26	3
$4p$–$7s$	8841	+0·21	3
	8828	+0·21	3
$4p$–$4d$	16750	+0·21	2
	16719	+0·18	2
	16763	+0·07	1
$5s$–$6p$	17699	+0·06	

lines which is 0·32 dex smaller than the present abundance. In view of the neglect of additional opacity the agreement is considered satisfactory.

As well as the Al I lines in Table V, a few additional lines were listed by Eriksson and Isberg or appear in the RRT. A supplementary table will not be given here: weak lines from the transitions $3d$–$6p$, $4p$–$8s$ and $4p$–$7d$ are probably present in the solar spectrum, and certain stronger lines are identified in the ultraviolet spectrum, for example $3p^2P^0$–$3d^2D$. An extrapolation from the results of Table V suggests that the transition $3d$–$9f$ should be detectable in the solar spectrum. The equivalent widths for the two lines are estimated at 10 and 7 mÅ. Their laboratory wavelengths are not available but the position of the $9f^2F^0$ level may be established by extrapolation. The predicted wavelengths are 6906·29 and 6905·65 Å. The latter is masked by a telluric line. The former may be identified with a 5 mÅ line at λ 6906·27, which in the RRT is assigned the identification Al I? The line is markedly weaker than is predicted. It is of interest to note that a similar result is obtained for $3d$–$8f$ (see Table VI).

The line at λ 3900·660, identified in RRT as Al II?, arises from the transition $3s(^2S)3p\,^1P^0$–$3p^2\,^1D$. Unfortunately, an accurate oscillator strength cannot be calculated for this transition. In order to evaluate an approximate radial integral by semi-empirical methods, it will be assumed that the transition is of the type $3p(^2P)3s$–$3p(^2P)^3p$. Intermediate coupling calculations for Mg I (Cowan & Warner unpublished) show that the $3p^2\,^1D$ state is considerably mixed with several of the $3snd\,^1D$ terms, and it may be assumed that Al II will be similarly mixed. Adopting the Mg I mixing coefficients and the radial integral determined in the above fashion, it is found that $gf \sim 1{\cdot}1$. This gives a predicted equivalent width of 62 mÅ.

Since the observed equivalent width is 20 mÅ it may be concluded that this line is almost certainly due to Al II. The astrophysical oscillator strength for λ 3900·16 is $gf = 0{\cdot}15$.

4. *Phosphorus*

4.1 *Introduction.* In a recent discussion of phosphorus lines in the solar spectrum Swensson (1966) lists 26 lines due to P I. Details of 13 lines, which appear unblended in the solar spectrum, are given in Table VII. Swensson's identification for four lines is rejected (see below) and for the remaining nine lines equivalent width measurements are made difficult by the presence of neighbouring lines.

TABLE VII

P I lines in the solar spectrum

Transition	Multiplet	Δj	$\lambda_\odot$	χ	log gf	W_λ L	W_λ Mo	W_λ M	log W/λ +7
$3p^2 4s$–$3p^2 4p$	^4P–$^4D^0$	5/2–7/2	10581·56	6·98	0·45	23		30	1·34
		3/2–5/2	10529·58	6·95	0·17	15		18	1·16
		1/2–3/2	10511·62	6·93	−0·23	6·6		9	0·80
		3/2–3/2	10681·41	6·95	−0·12	7·5:		11	0·84
		3/2–1/2	10769·41	6·95	−0·92	1·0			−0·03
$3p^2 4s$–$3p^2 4p$	^4P–$^4P^0$	5/2–5/2	9796·82	6·98	0·19	14		18	1·16
		3/2–1/2	9750·75	6·95	−0·21	5·5			0·75
$3p^2 4s$–$3p^2 4p$	^4P–$^4S^0$	5/2–3/2	9525·75	6·98	−0·12	6·6:			0·84
	^2P–$^2D^0$	3/2–5/2	11183·20	7·21	0·35	10·5			0·97
	^2P–$^2P^0$	1/2–1/2	9903·70	7·17	−0·28	2·6			0·42
		3/2–1/2	10204·70	7·20	−0·58	2·0			0·29
	^2P–$^2S^0$	3/2–1/2	16483·24	7·21	−0·46		8		0·69
		1/2–1/2	15711·47	7·17	−0·76		4		0·41

4.2 *Oscillator strengths.* There are no experimental oscillator strengths in phosphorus for the lines observed in the Sun. The lines in Table VII all arise from the transition array $3p^2 4s$–$3p^2 4p$. Comparison of the term splittings (Martin 1959) in ^4P and ^2P of $3p^2 4s$ shows that this configuration is extremely close to being LS-coupled. In $3p^2 4p$ the levels lie very close together and some mixing by spin–orbit interaction is to be expected. $4p^4 D^0$ appears fairly pure, but $4p^4 P_{3/2}{}^0$ is perturbed by neighbouring terms. The observed intercombination lines in this transition array are all $4s^4 P$–$4p^2 D^0$, which suggests that $4p^2 D^0$ is mixed with $4p^4 P^\circ$ and $4p^4 S^0$. Hence, it was decided not to accept any ' permitted ' transitions going to $4p^4 P_{3/2}{}^0$ or $4p^2 D^0$.

It is interesting to note that the one line λ 11 183·20 in Table VII, which is rejected on these grounds, gives a smaller abundance than the other lines in the array (see Fig. 3). Three transitions going to $4p^4 P_{3/2}{}^0$ should be present in the solar spectrum. Swensson shows that one is masked and the other two are blended with CN lines. The solar line at λ 9976·71 with an equivalent width of not more than 3 mÅ is the strongest line within ±0·5 Å of the laboratory wavelength for the P I line. Since the predicted equivalent width assuming LS coupling is 6 mÅ, it is clear without subtracting the contribution of the CN line that the f-value for this line is in error by at least a factor two. The other solar line at λ 9563·56 with an observed equivalent width of about 6 mÅ is wholly attributable to the CN line

(1, 0)$P_1(36)$ λ 9563·559, predicted W_λ = 5·8 mÅ (Lambert 1967b). The P I line has a laboratory wavelength λ 9563·45 and may be presumed masked by telluric absorption.

The behaviour of both λ 11 183·20 and λ 9976·71 is as expected because these lines calculated in intermediate coupling would have *f*-values smaller than those given in LS-coupling.

4.3 *Abundance.* The composite curve of growth is shown in Fig. 3. The scatter about the mean curve of growth is small and the most discrepant point is due to the line λ 11 183·20. This line is rejected (see previous section) and the two weak lines $4s^2P$–$4p^2S^0$ at about 16 000 Å are given half weight in the abundance determination. The mean abundance is

$$\log \frac{N_P}{N_H} = -6{\cdot}57 = 5{\cdot}43 - 12{\cdot}00.$$

This abundance is 0·09 dex larger than the GMA value. A probable error of about ±0·02 is estimated from abundance estimates for individual lines. This estimate does not include the larger errors attributable to uncertainties in the model atmosphere.

4.4 *Discussion.* The revised abundance and the coulomb approximation oscillator strengths may be used to compute the predicted equivalent widths for other P I lines. Suggested identifications for P I lines in the solar spectrum may be tested through a comparison of the predicted and observed equivalent widths.

This test applied to Swensson's identifications indicates that four of his new identifications should be withdrawn. Two other lines which appear in the RRT should also be deleted. Details for these lines are summarized in Table VIII. Swensson concluded that lines from the *4s–5p* array were absent. This is confirmed by the predictions; the strongest line has a predicted intensity of only 0·12 mÅ.

The identification of these weak P I lines may be achieved when low noise scans of the solar spectrum are available, but improved laboratory wavelengths will be necessary for an unambiguous identification.

TABLE VIII

A comparison between the observed and predicted equivalent widths for six P I lines

Solar data		P I data				Identification
$\lambda_\odot$	W_λ	λ	W_λ (pred.)	Multiplet	Δj	
11095·25	2	5·2	0·20	$4p^2S^0$–$5s^2P$	1/2–3/2	
11485·88	3	5·8	0·07		1/2–1/2	Si I†
8741·71	1·4	1·61	0·47	$4p^2S^0$–$4d^2P$	1/2–3/2	CN*
8637·56	1	7·61	0·23		1/2–1/2	
7175·316	7·5	5·12	0·30	$4p^4D^0$–$5d^4F$	7/2–9/2	Atmospheric H_2O
7176·59	2	6·66	0·20		5/2–7/2	

* λ 8741·678 (4, 2) Q_2 (53); predicted W_λ = 1·3 mÅ (Lambert 1967b).
† λ 11485·83 $4p^1D_2$–$4d^1F_3^0$.

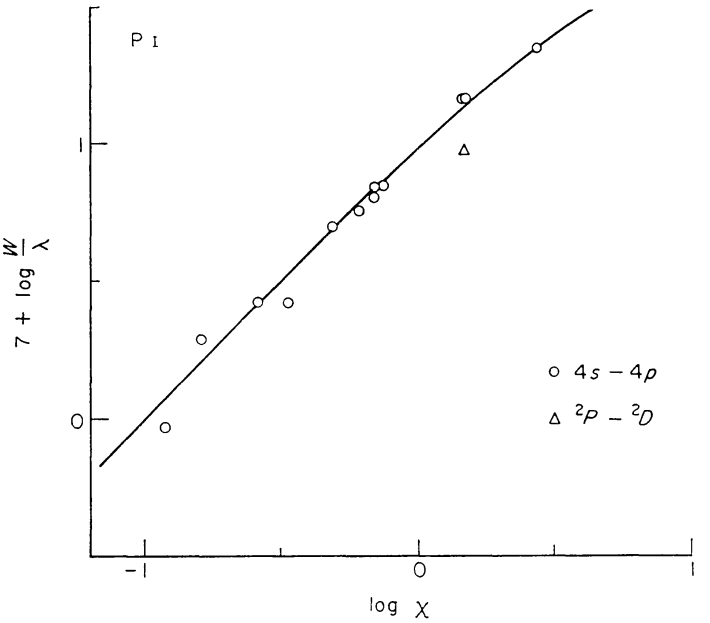

FIG. 3. *Curve of growth for the 4s–4p transition array in P* I.

5. *Sulphur*

5.1 *Introduction.* A catalogue of S I lines in the solar spectrum between 4000 and 25 500 Å is given in Table IX. Interparental transitions are not included (but see Section 5.4). For $\lambda \leqslant 9200$ Å, this compilation is based on the predicted wavelengths derived from the term analysis by Moore (1945) with revisions by Toresson (1960). Laboratory wavelengths given by Frerichs (1933) and Meissner, Bartelt & Eckstein (1933) were also referred to and are quoted for certain multiplets for which the predicted wavelengths are in apparently poor agreement with the solar wavelengths. For $\lambda \geqslant 9200$ Å, the laboratory wavelengths given by Jakobsson (1967) are adopted.

In Table IX, 103 lines are identified as due to S I (this total includes the tentative identifications but excludes the assignments of S I as a contributor to a blend), and 43 are believed to represent new identifications. It is of interest to record that 50 S I lines occur in the wavelength interval covered by the Delbouille & Roland Atlas (λ 7498–12016), and of these 27 are new identifications.

A few notes are required to supplement Table IX. In the case of a blend with a CN line, the predicted equivalent width for the CN line (Lambert 1967b) was subtracted from the total observed equivalent width. An identification is given in parenthesis when it appears to be a minor contributor to a blend. The identification S I? indicates that the assignment is doubtful on account of a wavelength or equivalent width discrepancy.

There is a clear and urgent need for a remeasurement of the S I spectrum in the interval $\lambda < 9200$ Å. This would undoubtedly serve to clarify many of the tentative identifications and should enable a number of new identifications to be given.

The forbidden lines of S I arising from transitions within the $3p^4$ ground configuration are the subject of a separate investigation (Lambert & Swings 1967).

5.2 *Oscillator strengths.* The observable transitions in S I are of the type $3p^3n'l'–3p^3n''l''$. Although basically a four-electron spectrum considerable simplification results because $3p^3$ is a half-closed shell and, therefore, the spin–orbit

Table IX

S I lines in the solar spectrum

Transition array	Multiplet	Δj	λ_{air}	$\lambda_\odot$	χ	log gf	L	W_λ PPO/M	log W_λ/λ	Ident.	Ref.	Notes
$3p^3(^4S^0)4s$–$3p^3(^4S^0)4p$	$^5S^0$–^5P	2–3	9212·865	2·838	6·52	+0·38	166		2·26	S I, Atm.	BM	
		2–2	9228·092	8·101		+0·23	135	139	2·17	S I	BM	
		2–1	9237·538	7·56		−0·01	116	111	2·09	S I	BM	
	$^3S^0$–^3P	1–2	10455·451	5·455	6·86	+0·25	130	130*	2·09	S I	BM	
		1–1	10456·757	6·753		+0·03	106	107*	2·01	S I	BM	
		1–0	10459·406	9·436		−0·44	65	70*	1·81	S I	BM	
$3p^3(^4S^0)4s$–$3p^3(^4S^0)5p$	$^5S^0$–^5P	2–3	4694·13	4·117	6·52	−1·39		12	1·41	S I	RRT	
		2–2	4695·44	5·446		−1·54		8	1·23	S I	RRT	
		2–1	4696·25	6·262		−1·76		8	1·23	S I	RRT	
	$^3S^0$–^3P	1–2	5278·91	8·961	6·86	−1·70		6·5	1·03	S I	RRT	
		1–1	5278·60	8·577		−1·92		2	0·58	S I	New	
		1–0	5278·04			−2·39						(1)
$3p^3(^4S^0)4p$–$3p^3(^4S^0)3d$	^5P–$^5D^0$	3–4	22707·738	8·31	7·87	+0·41		86†	1·58	S I	JAK	
		3–3	22644·090			−0·18						(2)
		3–2	22655·455	6·07		−1·04		24†		CH_4(S I)	MO	
		2–3	22552·612	2·74		+0·12		82†	1·40	S I, N_2O	JAK	(3)
		2–2	22563·867			−0·09						(2)
		2–1	22575·431	5·56		−0·67		52†	1·01	S I, N_2O	JAK	(3)
		1–2	22507·592	7·63		−0·31		34†	1·18	S I	New	(4)
		1–1	22519·105	9·17		−0·20		38†	1·23	S I, (N_2O)	JAK	
		1–0	22526·053	5·96		−0·55		10†	0·65	S I?	JAK	
	^3P–$^3D^0$	1–1	18949·711	9·92	8·05	−0·33		14†	0·87	S I	New	(5) (6)

$3p^3(^4S^0)4p$–$3p^3(^4S^0)4d$	^5P–$^5D^0$	3–4	8694·71	4·641	7·87	+0·03	31	34	1·57	S I	RRT
		3–3	8693·99	3·958		−0·56	12	17	1·14	S I	RRT
		3–2	8693·14	3·15		−1·42	1·7	3	0·36	S I	RRT
		2–3	8680·46	0·405		−0·26	25:	25	1·46	S I	RRT
		2–2	8679·60	9·646		−0·46		41		Fe I, S I	RRT
		2–1	8678·94	8·950		−1·05	8·3	8	0·94	S I, CN	RRT
		1–2	8671·35	1·308		−0·69	10	6	1·06	S I	RRT
		1–1	8670·68	0·627		−0·58	11·6	12	1·13	S I	RRT
		1–0	8670·24	0·20		−0·93	5·7	8	0·82	S I	RRT
	^3P–$^3D^0$	2–3	9035·92	5·88	8·05	−0·66	5·6:		0·79	S I	New
		2–2	9039·29	9·25		−1·41	1·5:		0·22	S I	New
		2–1	9039·71	9·70		−2·58	<1				Absent
		1–2	9036·30	6·35		−0·93	2·9		0·51	S I	New
		1–1	9036·72	6·72		−1·41	5·4			Fe I, S I	New
		0–1	9038·74	8·79		−1·28	6·5			Fe I, S I	New
$3p^3(^4S^0)4p$–$3p^3(^4S^0)5d$	^5P–$^5D^0$	3–4	6757·16	7·195	7·87	−0·40		19	1·45	S I	RRT
		3–2, 3	6756·98	7·08		−0·94		5:	0·87	S I?	New
		2–2, 3	6748·79	8·870		−0·48		17	1·40	S I, (Cr I)	New (7)
		2–1	6748·57	8·65		−1·48		5:	0·87	S I?	New
		1–2	6743·79	3·89		−1·12		2·5:	0·57	S I	New
		1–0, 1	6743·58	3·575		−0·85		12	1·25	S I	RRT
	^3P–$^3D^0$	2–3	7244·72	4·850	8·05	−0·74		63		Ti I, (S I)	RRT
		2–2	7244·96			−1·49					
		2–1	7244·33			−2·66		<2			Absent
		1–2	7243·09	3·09		−1·01		6	0·92	S I	RRT
		1–1	7242·41	2·41		−1·49		3	0·62	S I	RRT
		0–1	7243·71	3·72		−1·39		88		Atm, (S I)	(New)

1968MNRAS.138..181L

TABLE IX (*continued*)

Transition array	Multiplet	Δj	λ_{air}	$\lambda_\odot$	χ	log gf	W_λ L	W_λ PPO/M	log W_λ/λ	Ident.	Ref.	Notes
$3p^3(^4S^0)4p-3p^3(^4S^0)6d$	$^5P-^5D^0$	3–	6052·66	2·682	7·87	−0·63		11	1·26	S I	RRT	
		2–	6046·04	6·015:		−0·78		16		S I?	RRT	
		1–	6041·93	1·93		−1·00		3·5	0·78	S I	RRT	
	$^3P-^3D^0$	2–3	6538·57	8·538	8·05	−0·91		6	0·96	S I, Atm.	RRT	
		2–2	6537·97	7·938		−1·66		2·5		Cr I, (S I)	(New)	
		2–1	6537·18			−2·83		<2				Absent
		1–2	6536·41	6·47		−1·18		3:	0·66	S I?	New	
		1–1	6535·62	5·60		−1·66		2·5	0·56	S I?	New	
		0–1	6536·68	6·720		−1·53		8		Atm, (S I)	(New)	
$3p^3(^4S^0)4p-3p^3(^4S^0)7d$	$^5P-^5D^0$	3–	5706·11	6·108	7·87	−0·89		25		Fe I, S I	New	
		2–	5700·24	0·289		−1·04		15		Cu I, S I	New	
		1–	5696·65	6·652		−1·26		3·5		S I	RRT	
	$^3P-^3D^0$	2–3	6175·85		8·05	−1·07	<2					Absent
		1–2	6173·57	3·571		−1·34	2·5:		0·16	S I	New	
		1–1	6172·80	2·734		−1·82	1·5		0·38	S I?	New	
$3p^3(^4S^0)4p-3p^3(^4S^0)8d$	$^5P-^5D^0$	3–	5507·00	6·992	7·87	−1·11		7	1·10	S I	RRT	
		2–	5501·53	1·477		−1·26		115		Fe I, (S I)	(New)	
		1–	5498·18	8·189		−1·46		2·5	0·66	S I, Fe II	RRT	
	$^3P-^3D^0$	2–3	5961·20	1·228	8·05	−1·23		2:	0·53	S I	New	
$3p^3(^4S^0)4p-3p^3(^4S^0)5s$	$^5P-^5S^0$	1–2	13776·556	6·74	7·87	−0·28		25†	1·26	S I	JAK	(6)
	$^3P-^3S^0$	2–1	15478·485	8·79	8·05	−0·05		110†	1·85	S I, (H_2O)	JAK	
		1–1	15469·813	0·05		−0·25		58†	1·57	S I	JAK	
		0–1	15475·615	5·63		−0·72		60†	1·59	S I?	JAK	

$3p^3(^4S^0)4p-3p^3(^4S^0)6s$	$^5P-^5S^0$	3–2	7696·70	6·72	7·87	−0·92		2·5:	0·51	S I	RRT	
		2–2	7686·09	6·13		−1·07	4·3	6	0·75	S I	RRT	
		1–2	7679·62	9·60		−1·29	2·0	4	0·41	S I	RRT	
	$^3P-^3S^0$	2–1	8452·19	2·086	8·05	−1·05	5·6	5	0·82	S I, Atm	RRT	
		1–1	8449·57	9·50		−1·27	1·7		0·30	S I	New	
		0–1	8451·34			−1·74	<1					Absent
$3p^3(^4S^0)4p-3p^3(^4S^0)7s$	$^5P-^5S^0$	3–2	6415·49	7·87		−1·40		3	0·57	S I?, CN	New	
$3p^3(^4S^0)3d-3p^3(^4S^0)5p$	$^5D^0-^5P$	4–3	16542·665	2·87	8·42	−0·31		12†	0·86	S I	Mo	
		3–3	16576·63	6·74		−0·92		9†	0·73	S I	JAK	
		3–2	16593·191	3·30		−0·62		15†		S I, Ti	New	(8)
		2–3	16570·53			−1·78		<3†				Absent
		2–2 0–1	16587·118	7·44		−0·70		28†	1·23	S I?	Mo	
		2–1	16597·23	7·39		−1·05		3†	0·25	S I	JAK	
		1–2	16580·86	0·83		−1·41		3†	0·25	S I?	New	
		1–1	16590·956	1·13		−0·94		15†	0·96	S I?	Mo	
	$^3D^0-^3P$	3–2	24415·85	6·11	8·70	−0·19		8†	0·51	S I	JAK	(9) (6)
$3p^3(^4S^0)3d-3p^3(^4S^0)4f$	$^5D^0-^5F$	4–	11390·122	0·14	8·42	+0·69	49		1·63	S I	New	
		3–	11406·195			+0·58						(2)
		2–	11403·283	3·22		+0·43	19:		1·22	S I	New	
		1–	11400·303	0·35		+0·21	32		1·44	S I?	New	
		0–1	11398·492	8·50		−0·27	8:		0·85	S I	New	
	$^3D^0-^3F$	3–	15422·255	2·51	8·70			99†	1·81	S I	JAK	
		2–	15403·762	3·99				84†	1·61	S I, CO_2	JAK	(3)
		1–	15400·057	0·12				82†	1·73	S I	JAK	

1968MNRAS.138..181L

1968MNRAS.138..181L

TABLE IX (*continued*)

Transition array	Multiplet	Δj	λ_{air}	$\lambda_\odot$	χ	log gf	W_λ L	W_λ PPO/M	log W_λ/λ	Ident.	Ref.	Notes
$3p^3(^4S^0)3d$–$3p^3(^4S^0)5f$	$^5D^0$–^5F	4–	8874·50	4·478	8·42	+0·20	13		1·17	S I	BM	
		3–	8884·29	4·24		+0·09	13		1·17	S I	BM	
		2–	8882·56	2·50		−0·06	7·1		0·90	S I	BM	
		1–	8880·76	0·69		−0·28	3·8		0·63	S I	BM	
		0–1	8879·73	0·60		−0·76	1·5		0·23	S I	New	
	$^3D^0$–^3F	2–	11135·373	5·40	8·70	−0·03	7·6:		0·83	S I	New	(6)
$3p^3(^4S^0)3d$–$3p^3(^4S^0)6f$	$^5D^0$–^5F	4–	7923·85	3·81	8·42	−0·14	5·3:	3	0·75	S I, CN	RRT	
		3–	7931·70	1·772		−0·25		5		Atm, S I	RRT	
		2–	7930·33	0·28		−0·40	3·0	2	0·50	S I, CN	RRT	
		1–	7928·84	8·80		−0·62	2:		0·40	S I	New	
		0–1	7928·28	8·24		−1·10		2		Atm, (S I)	(New)	
$3p^3(^2D^0)4s$–$3p^3(^2D^0)4p$	$^3D^0$–^3D	3–3	9649·568	9·55	8·41	+0·32	23		1·38	S I, Atm	New	
		3–2	9697·408	7·40		−0·59	6·0		0·59	S I, CN	New	
		2–3	9633·130	3·20		−0·59	8·1		0·52	S I, CN	New	
		2–2	9680·809	0·85		+0·06	16:		1·22	S I	New	
		2–1	9680·561			−0·60						(2)
		1–2	9672·531	2·55		−0·60	2·1:		0·34	S I	New	
		1–1	9672·283	2·30		−0·12	8·6:		0·95	S I	New	
	$^3D^0$–^3P	3–2	8668·456	8·45	8·41	+0·19	6·7	9	0·89	S I	New	
		2–2	8655·17	5·20		−0·56		2	0·36	S I	New	
		2–1	8633·19	3·15		−0·08	4·3		0·70	S I	New	
		1–2	8633·54			−1·73	<1					Absent
		1–1	8626·60	6·59		−0·56	5·0:	5	0·60	S I, CN	New	
		1–0	8617·15	7·15		−0·43	1·5:		0·24	S I	New	

$^3D^0$–^3F	2–2	9445·05	5·05	8·41	−0·56	16		CN, S I	New	(6) (10) (11)
	1–2	9437·16	7·15		+0·16	8	0·93	S I	New	(11)
$^1D^0$–^1F	2–3	10635·993	5·981	8·58	+0·37	26	1·39	S I	JAK	
$^1D^0$–^1P	2–1	11601·768	1·75	8·58	0·00	11:	0·98	S I	New	

References:

BM = Babcock & Moore (1947), JAK = Jakobsson (1967), Mo = Mohler (1955), RRT = Moore, Minnaert & Houtgast (1966), and New = new identifications.

Notes to Table I:

(1) The S I line is probably present between the solar lines λ 5277·812 and λ 5278·70.
(2) The S I line is masked by strong telluric absorption lines.
(3) For log W_λ/λ the predicted W_λ for the telluric component (Mohler 1955) was subtracted out.
(4) Mohler (1955) gives the identification as Ti I but the curve of growth (Fig. 8) suggests that S I is the principal contributor.
(5) W_λ uncertain because of telluric H_2O lines.
(6) Other members of the multiplet masked by strong telluric features.
(7) The identification (λ 6748·779, W_λ = 5 mÅ) in the RRT is discarded.
(8) Mohler (1955) suggests that Ti I and Ni I contribute.
(9) Mohler (1955) suggests the identification C I $5p^3D_3$–$8d^3F_3^0$ but the predicted wavelength from the revised energy levels (Johansson 1966) is λ 24400·8 ± 0·6 Å.
(10) The predicted W_λ for the CN line is 12 mÅ, and, therefore, S I is the minor contributor.
(11) Identifications based on predicted S I wavelengths. For $4s'\ ^3D^0$–$4p'\ ^3D$ the predictions were not in accord with Jakobsson's accurate wavelengths; differences of 0·3 to 0·5 Å were found. This discrepancy suggests that these new identifications may be spurious.

* McMath–Hulbert measurement quoted by GMA.
† W_λ from Mohler (1955).
: Denotes uncertain measurement.

interaction constant ζ is zero. Thus, the only spin–orbit interaction that can occur is that resulting from the finiteness of $\zeta(n,l)$, and since ζ decreases rapidly with increasing n and l, there is very little mixing of levels within most configurations. This explains the almost complete absence of intercombination lines in the S I spectrum. Apart from $4p^5P$ and $5p^5P$, for which $\zeta(p)$ is large enough to be held responsible, all the term splittings in $3p^3nl$ must arise from the direct or indirect consequences of configuration mixing.

The $3p^3(^4S^0)3d^5D^0$ and $3p^3(^2D^0)4s^3D^0$ terms lie almost on top of each other and there is adequate evidence for level perturbations in both terms. Consequently $3d^5D^0$, which is the lower term of several transitions observed in the sun, will contain a large admixture of $4s^3D^0$. Similar arguments apply to $3d^3D^0$ and $4s^1D^0$. This strong mixing must also be primarily responsible for the strong observed interparental transitions of the type $3p^3(^4S^0)3d$–$3p^3(^2D^0)4p$.

Consequently the transitions $3p^3(^4S^0)3d$–$3p^3(^4S^0)nl$ and $3p^3(^2D^0)4s$–$3p^3(^2D^0)nl$ are excluded from the determination of the sulphur abundance. The term analysis indicates no strong *a priori* reasons for rejecting any of the other lines.

Coulomb approximation oscillator strengths are given in Table IX. Two series of experimental measurements are available for comparison. Bridges & Wiese (1966) report results for five multiplets. Results for three multiplets are given by Foster (1967). A comparison of the experimental and theoretical results is presented in Table X.

TABLE X

Experimental and theoretical oscillator strengths for S I

Multiplet	λ	CA	gf Bridges/Wiese	gf Foster
$4s^5S^0$–$4p^5P$	9212·9	2·41	1·9 ± 0·9	
	9228·1	1·72	1·5 ± 0·7	
	9237·5	1·03	0·9 ± 0·4	
$4s^5S^0$–$5p^5P$	4695	0·0875	0·04 ± 0·4	0·029 ± 0·005
$4s^3S^0$–$4p^3P$	10456	3·24	3·1 ± 1·5	
$4s^3S^0$–$5p^3P$	5279	0·0362	0·015 ± 0·007	0·013 ± 0·002
$4p^5P$–$4d^5D^0$	8685	2·95	3·4 ± 1·7	
$4s^3S^0$–$4p'^3P$	4155			0·019 ± 0·004

Two conclusions follow from this table. First, the experimental results for the $4s$–$4p$ and $4p$–$4d$ transition arrays are in agreement to within the experimental error with the Coulomb approximation calculations. Second, the experimental results for the $4s$–$5p$ transition array are approximately a factor two less than the calculated values. Wiese & Bridges point out that the latter values should be considered uncertain owing to severe cancellation of the negative and positive contributions to the transition integral. The evidence from solar equivalent widths is examined in Section 5.4. The array $4s$–$5p$ is excluded for the purposes of the abundance determination. Inspection of the transition integrals for the higher members of the transition arrays $4p$–nd and $3d$–nf has shown no further cases of severe cancellation.

5.3 *Abundance.* Composite curves of growth which include the transitions deemed suitable for an abundance determination are shown in Figs 4–6. The abundances derived from the four multiplets in the transition arrays $4s$–$4p$ and

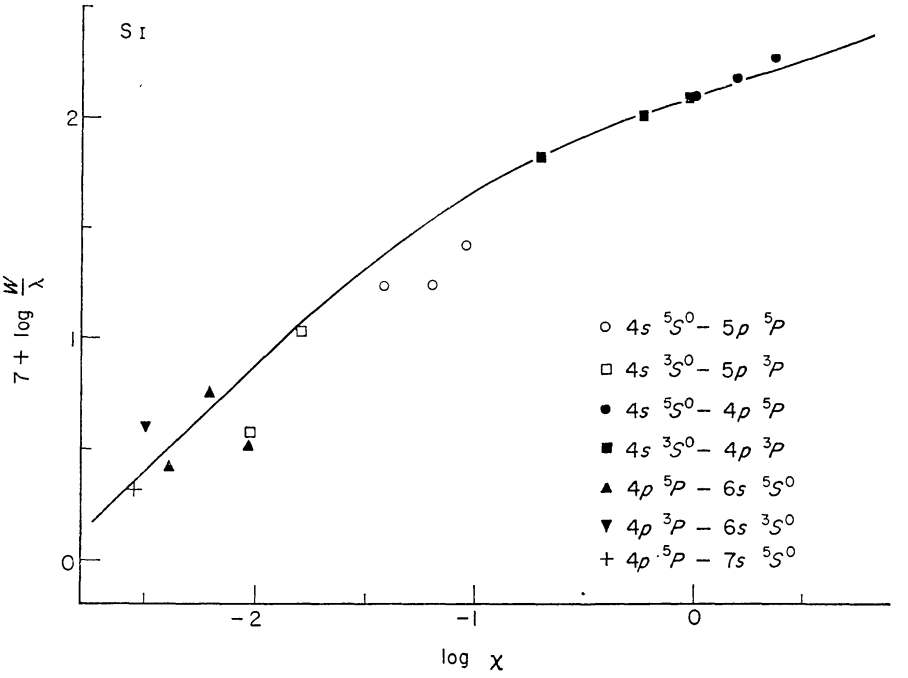

FIG. 4. *Curve of growth for ns–n'p transitions in S* I.

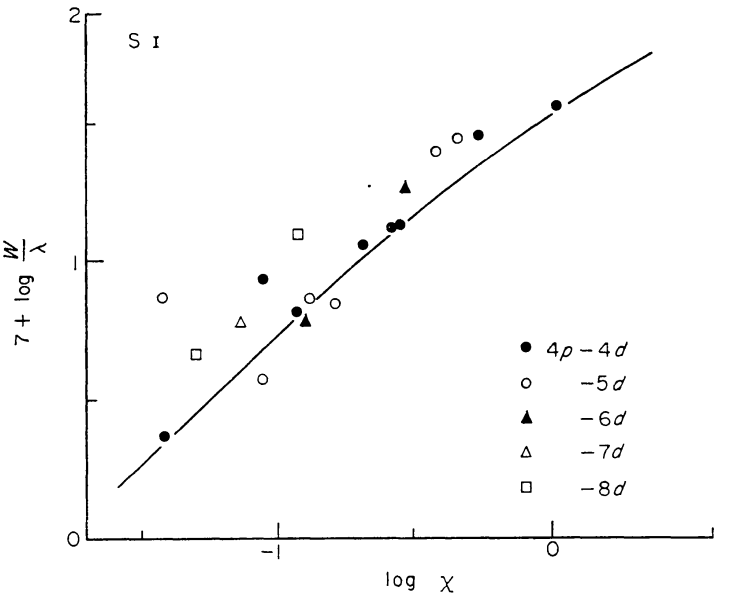

FIG. 5. *Curve of growth for* $4p^5P$–nd^5D^0 *transitions in S* I.

$4p$–$4d$ are summarized in Table XI. The results for individual multiplets are in very good agreement. Multiplet $4p^3P$–$4d^3D^0$ gives an apparently smaller abundance by 0·10 dex. The possibility of a misidentification owing to inaccurate wavelength predictions cannot be entirely ruled out. This multiplet is not included in the

derivation of the mean abundance. The 11 lines from the other three multiplets give

$$\log \frac{N_S}{N_H} = -4{\cdot}79 = 7{\cdot}21 - 12{\cdot}00$$

or an abundance 0·09 dex smaller than the GMA value. The scatter of results from individual lines suggests an uncertainty of $\pm 0{\cdot}03$ dex.

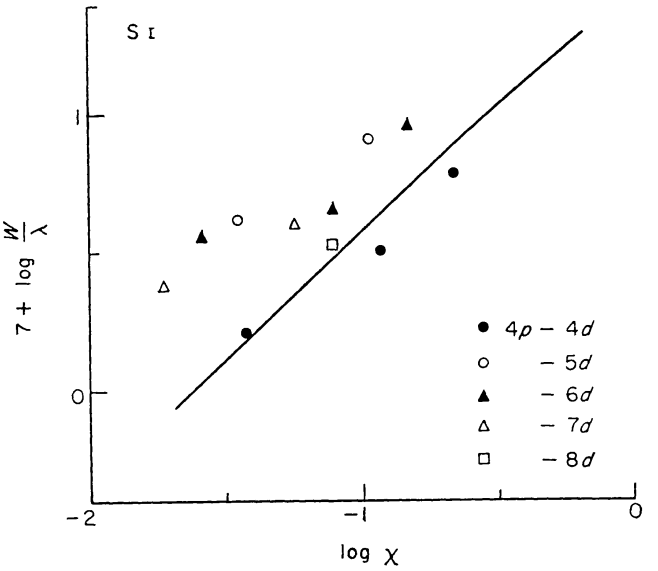

FIG. 6. *Curve of growth for* $4p^3P$–nd^3D^0 *transitions in S* I.

For the higher members of the series $4p$–nd, the curves of growth (Figs 5 and 6) show that the observed equivalent widths are apparently systematically greater than is predicted with the revised abundance. For example, the mean abundance from the transitions $4p$–nd with $n \geqslant 5$ is about 0·15 to 0·20 dex larger than the revised value. It is suggested that the discrepancy arises owing to errors in the equivalent widths for these faint lines. In particular, the present list must surely contain a number of spurious identifications resulting from the uncertainties in the predicted wavelengths. No weight can be attached to this discrepancy. Accurate laboratory wavelengths are urgently required.

The transition array $4p$–$5s$ occurs at 1·38 and 1·55 microns. The mean abundance from four lines is [S] = −0·02, which can be considered in agreement with the revised value.

5.4 *Discussion.* In Section 5.2, it was shown that the experimental measurements for the $4s$–$5p$ transition array were about a factor two smaller than the Coulomb approximation calculations. The identified lines from this array are included in Fig. 4 where the Coulomb approximation results are used. Clearly the observed equivalent widths are markedly weaker than is predicted. Agreement for the $4s^5S^0$–$5p^5P$ multiplet can be achieved through a reduction of the calculated oscillator strengths by a factor of about 0·5. The two lines from $4s^3S^0$–$5p^3P$ indicate that a similar reduction is required. The conclusion is that the solar equivalent widths confirm the experimental measurements of the oscillator strengths. A similar conclusion was reached by Foster (1967).

TABLE XI

Results for the sulphur abundances from the leading member in the series 4s–np and 4p–nd

Multiplet	λ	[S]	log N_S/N_{17}
$4s^5S^0$–$4p^5P$	9220	−0·12	−4·82★
$4s^3S^0$–$4p^3P$	10460	−0·08	−4·78
$4p^5P$–$4d^5D^0$	8680	−0·08	−4·78†
$4p^3P$–$4d^3D^0$	9040	−0·18	−4·88

★ Omitting λ 9212 which gives [S] = +0·03 but is blended with a telluric line.

† Omitting λ 8678·94 and 8680·46 which give [S] = +0·18 and +0·02 respectively.

The transitions $3p^3(^4S^0)3d$–$3p^3(^4S^0)nf$, $-3p^3(^4S^0)np$, and $3p^3(^2D^0)4s$–$3p^3(^2D^0)4p$ were excluded for the purposes of an abundance determination because of perturbations resulting from the close proximity of the terms $3p^3(^4S^0)3d^5D^0$, $^3D^0$ and $3p^3(^2D^0)4s^5D^0$, $^3D^0$. The curves of growth shown in Figs 7–9 support the argument for their exclusion. The oscillator strengths for the transitions $3d$–nf are apparently about a factor three smaller than the calculated values given in Table IX. There is only a small variation with the principal quantum number n. The relative line strengths appear to have the LS coupling values. Similar results (Fig. 8) are obtained for the array $3p^3(^2D^0)4s$–$3p^3(^2D^0)4p$. The multiplets $^3D^0$–^3P, $^1D^0$–^1F, $^1D^0$–^1P indicate that the calculated oscillator strengths are too large by about a factor 2. The multiplets $^3D^0$–^3P and $^3D^0$–^3F indicate a somewhat larger factor (perhaps about four) but the possibility that some of the present identifications are spurious

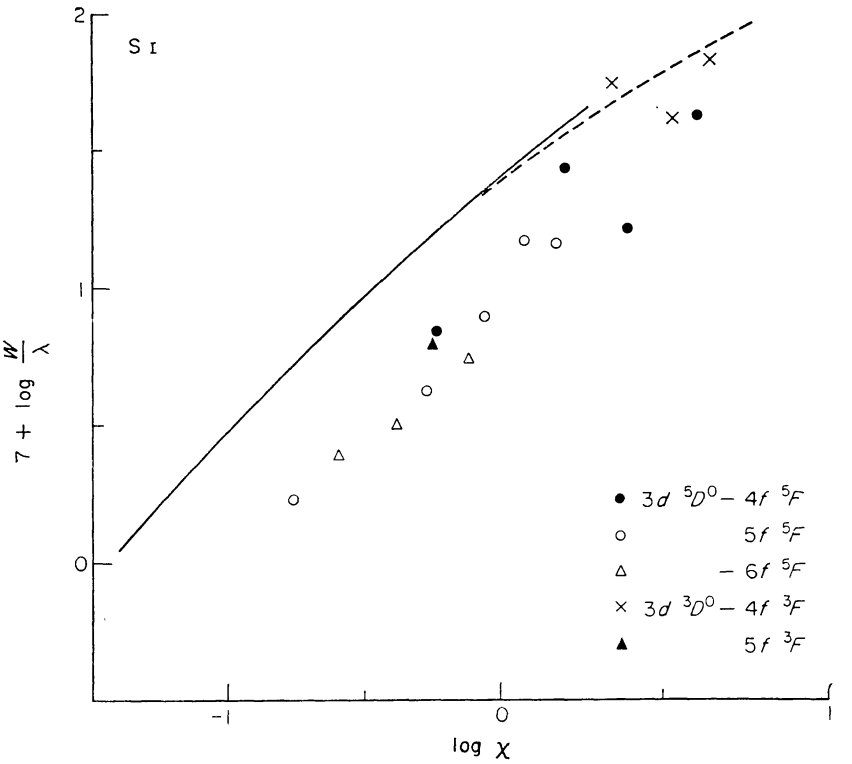

FIG. 7. *Curve of growth for 3d–nf transitions in S I. The solid line is the theoretical curve for* 11 000 Å *and* $\chi = 8{\cdot}40\ V$; *the dashed line is for* 15 400 Å *and* 8·70 *V.*

should not be overlooked. The proposed identifications for lines from the transition arrays $4p$–$3d$ and $3d$–$5p$ also give similar results and this is shown by Fig. 9. The scatter in Fig. 9 is probably attributable to errors in the adopted equivalent widths.

Figs 7–9 are presented to demonstrate the neccessity to select lines for which the Coulomb approximation and the assumption of LS coupling may be considered valid. Section 5.3 showed that if this selection is made, the abundance can be accurately determined. It may then be used to determine empirical or astrophysical

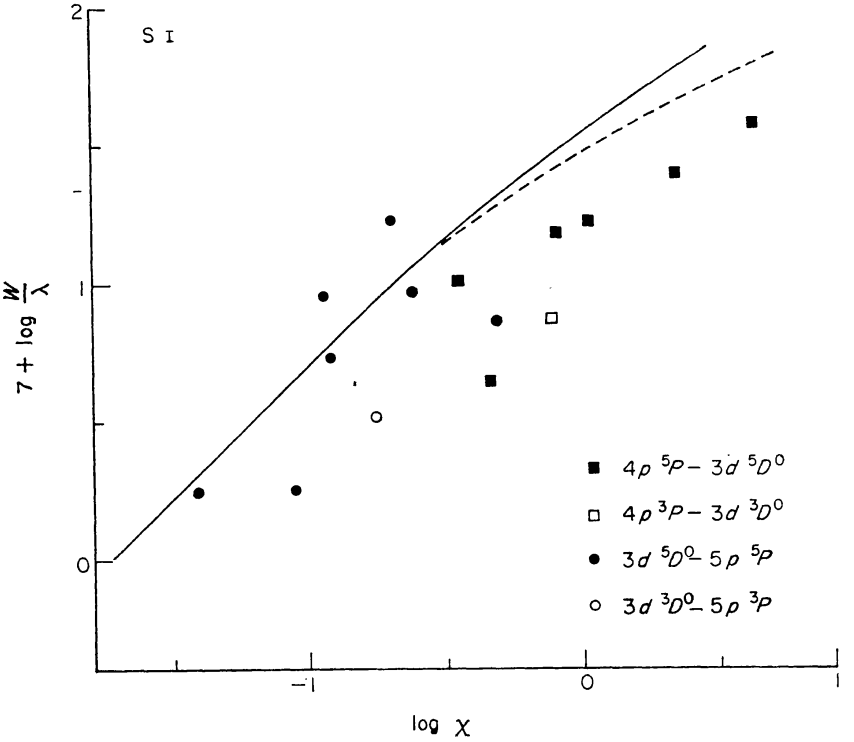

FIG. 8. *Curve of growth for 3d–np transitions in S* I. *The solid line is the theoretical curve for* 16 600 Å *and* $\chi = 8{\cdot}42$ *V; the dashed line is for* 22 500 Å *and* $\chi = 7{\cdot}87$ *V.*

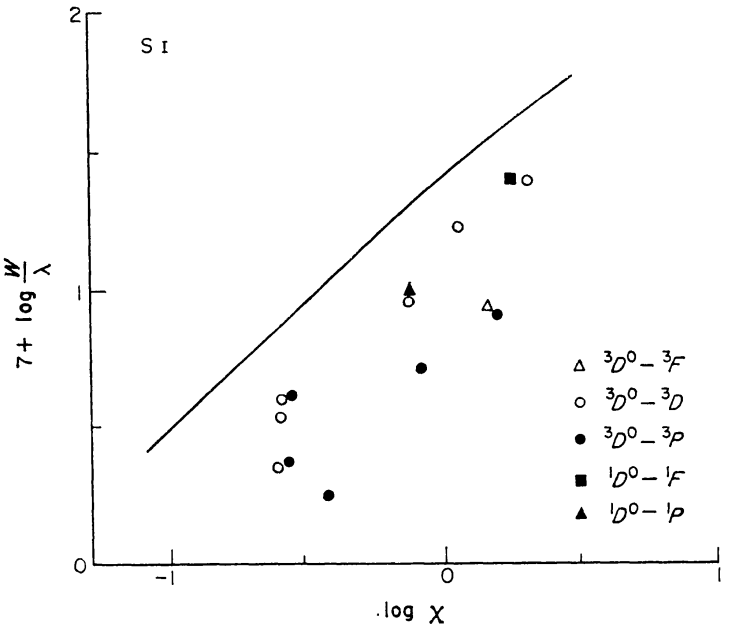

FIG. 9. *Curve of growth for the 4s′–4p′ transition array in S* I.

oscillator strengths for the rejected lines, which values may be used by theoretical spectroscopists to check improved calculations of the oscillator strengths.

It should be noted that a comparison of the wavelengths and the Delbouille and Roland Atlas indicates that certain interparental transitions might be present in the solar spectrum; for example $4s'\ ^3D_3$–$6p\ ^3P_2$ λ 9949·830 with W_λ = 4·1 mÅ. This comparison also enables an upper limit of about 1 to 2 mÅ to be assigned to the equivalent widths for a number of interparental transitions, for example, $4s'\ ^3D$–$6p\ ^3P$ λ 9932·359 and λ 9912·156. These equivalent widths could be readily converted to give a value for the oscillator strength for the transition.

6. *Potassium*

6.1 *Introduction.* Risberg (1956) listed the K I lines which are present in the solar spectrum between 4000 and 25 000 Å. A selection of nine lines are listed in Table XII. Certain lines are blended with telluric lines and must be discarded. Three weak lines, which are assigned the identification K I in the RRT, are also omitted and are discussed below.

TABLE XII

K I lines in the solar spectrum

Transition array	Multiplet	Δj	$\lambda_\odot$(Å)	χ	log gf	W_λ L	W_λ RRT	W_λ M	log W_λ/λ +7	Notes
$4s$–$4p$	^2S–$^2P^0$	1/2–1/2	7698·98	0·00	−0·16	149	154		2·29	
$4s$–$5p$	^2S–$^2P^0$	1/2–3/2	4044·15	0·00	−1·89		16	11	1·43	
		1/2–1/2	4047·23		−2·24		5	4	0·99	(1)
$4p$–$5s$	$^2P^0$–^2S	3/2–1/2	12522·16	1·62	−0·17			54	1·63	(2)
$4p$–$6s$	$^2P^0$–^2S	3/2–1/2	6938·74	1·62	−1·20		3		0·64	
$4p$–$7s$	$^2P^0$–^2S	3/2–1/2	5801·75	1·62	−1·69		1·5		0·41	
$4p$–$8s$	$^2P^0$–^2S	3/2–1/2	5339·70	1·62	−2·02		1		0·27	
$4p$–$3d$	$^2P^0$–^2D	3/2–3/2	11769·72	1·62	−0·45	33			1·45	
$4p$–$5d$	$^2P^0$–^2D	3/2–5/2	5831·94	1·62	−2·15		0·5		−0·07	

Notes to Table XII :

(1) Risberg (1956) incorrectly identified this line in the solar spectrum.

(2) W_λ from Mohler (1955). The solar identification proposed by GMA is incorrect. Risberg (1956) indicated that C I might be a contributor to this line but there is no C I line at this wavelength (Johansson (1966).

6.2 *Oscillator strengths.* The oscillator strengths were calculated in the same manner as for Na I. The $gf(4s$–$4p)$ given by the Coulomb approximation is 1·97 and by the STF method is 2·10. An accurate lifetime determination is in good agreement with these calculated values: $gf = 1{\cdot}97 \pm 0{\cdot}08$, (Stephenson 1951). An experimental measurement using the hook method gave $gf(4s$–$4p) = 2{\cdot}06$ (Ostrovskii & Penkin 1962). The inter-agreement of the theoretical and experimental results shows that the oscillator strength for the resonance lines is well determined.

The calculated oscillator strengths are adopted for the other transition arrays excepting $4s$–$5p$ and $4p$–$5d$. In these two cases, the dipole integral is especially sensitive to the effective quantum number. This is caused by the almost complete cancellation of the negative and positive contributions to the transition integral, and was remarked on by Bates & Damgaard (1949). For the transition array $4s$–$5p$, the ratio

$$gf(4s\text{–}4p)/gf(4s\text{–}5p) = 111{\cdot}5$$

as measured by Fillipov (1933) is adopted, and combined with the experimental measurement of $gf(4s–4p)$ given by Ostrovskii & Penkin (1962). For $4p–5d$ it happens that although the calculated oscillator strength is uncertain it is only two per cent larger than that measured by van der Held & Heierman (1936).

6.3 *Abundance.* In the composite curve of growth (Fig. 10) the selected lines fall close to a single curve of growth. The potassium abundance is

$$\log \frac{N_K}{N_H} = -6{\cdot}95 = 5{\cdot}05 - 12{\cdot}00.$$

The scatter in Fig. 10 corresponds to an abundance uncertainty of about $\pm 0{\cdot}10$ dex. This present result is 0·35 dex (or a factor 2·2) larger than the GMA value. It should be noted that owing to a combination of factors their abundance was most

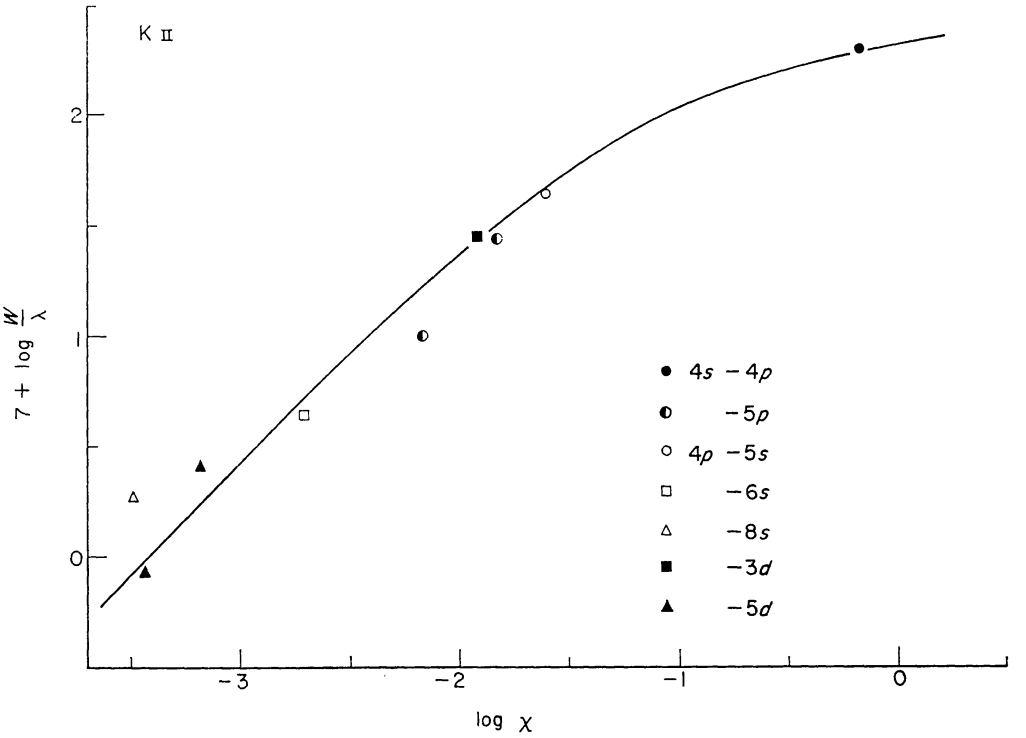

FIG. 10. *Curve of growth for K* I.

uncertain. Firstly, for the transition $4s–5p$ GMA adopted the Coulomb approximation oscillator strengths but these are most uncertain as a result of severe cancellation. The experimental measurements are about 0·25 dex smaller. Secondly, for the strong line $4s–4p$ λ 7698 they assumed damping to be zero. Thirdly, one line to which they attach little weight was incorrectly identified. Finally, their use of a single curve of growth computed for an average wavelength and an Fe I line may have introduced a small error.

6.4 *Discussion.* In Table XIII, the observed and predicted equivalent widths are compared for the three weak lines, which are assigned the identification K I in the RRT but which were omitted from Table XII. The observed intensities exceed the predictions by about a factor four. This discrepancy indicates that the K I identification is questionable.

TABLE XIII

Comparison between the observed and predicted equivalent widths for three K I lines

Multiplet	Δj	λ	$\lambda_\odot$	W_λ	W_λ (predicted)
$4p^2P^0$–$5d^2D$	1/2–3/2	5812·146	2·131	1	0·2
$4p^2P^0$–$6d^2D$	3/2–5/2	5359·574	9·528	2	0·3
$4p^2P^0$–$7s^2S$	1/2–1/2	5782·384	2·371	3	0·7

7. *Concluding remarks*

The abundances obtained in the present study are summarized in Table XIV which includes the GMA values for comparison, which values are given in the most recent compilation of photospheric abundances (Müller 1967).

TABLE XIV

The abundances: a summary and comparison with GMA

Element	Abundance $\log N$ with $\log N_H = 12·00$	
	This paper	GMA
Na	6·18	6·30
Al	6·40	6·20
P	5·43	5·34
S	7·21	7·30
K	5·05	4·70

It is difficult to give a quantitative estimate of the accuracy of these determinations but the uncertainty $\pm 0·10$ dex or less is indicated. The results for Na, Al and K are approximately independent of the adopted model atmosphere. The detailed discussion for Na indicated that a further reduction in the abundance by, perhaps, 0·10 dex, might be necessary. For Al, the approximate treatment for mixing in the $3d$ level reduces but does not eliminate the difference in the abundances obtained from the $4p$–ns and $3d$–nf series. A further correction of about 0·10 dex might be anticipated.

The abundance of P and S is based on high excitation lines which are more sensitive to temperature errors in the model atmosphere. It should be noted that the present model does not attempt to represent the solar granulation. It can be shown that owing to the presence of granulation, the present abundances are likely to be overestimated by about 0·05 dex. An investigation of the centre–limb variation of the line profiles of weak high excitation lines would be of great interest.

Acknowledgments. During this work Warner has been supported by the Radcliffe–Henry Skynner Fellowship at Balliol College, Oxford.

Department of Astrophysics,
Oxford
1967 *July.*

References

Allen, C. W., 1936. *Mon. Not. R. astr. Soc.*, **96**, 843.
Aller, L. H., 1963. *The Atmospheres of Sun and Stars*, Ronald Press, New York.
Anderson, E. M. & Zilitis, V. A., 1964. *Opt. Spectrosc.*, **16**, 99.

Babcock, H. D. & Moore, C. E., 1947. *The Solar Spectrum* λ 6600–λ 13495, Carnegie Institute, Washington.
Bates, D. R. & Damgaard, A., 1949. *Phil. Trans. R. Soc.*, A**242**, 101.
Bridges, J. M. & Wiese, W. L., 1966. *Trans. Int. astr. Un.*, **XIIB**, 175.
Chamaraux, P., 1967. *Ann. Astrophys.*, **30**, 67.
Delbouille, L. & Roland, G., 1963. *Photometric Atlas of the Solar Spectrum from* λ 7498 *to* λ 12016, Liège.
Demtroder, W., 1962. *Z. Phys.*, **166**, 42.
Eriksson, K. B. S. & Isberg, H. B. S., 1963. *Ark. Fys.*, **23**, 527.
Fillipov, A. N., 1933. *Zh. eksper. teor. Fiz.*, **3**, 520.
Foster, E. W., 1967. *Proc. phys. Soc.*, **90**, 275.
Frerichs, R., 1933. *Z. Phys.*, **80**, 150.
Froese, C., 1967. Personal communication.
Goldberg, L., Müller, E. A. & Aller, L. H., 1960. *Astrophys. J., Suppl. Ser.*, **5**, 1.
Griem, H. R., 1964. *Plasma Spectroscopy*, McGraw-Hill, New York.
van der Held, E. F. M. & Heierman, J. H., 1936. *Physica*, **3**, 31.
Holweger, H., 1967. *Z. Astrophys.*, **65**, 365.
Hulpke, E., Paul, E. & Paul, W., 1964. *Z. Phys.*, **177**, 257.
Hunger, K., 1960. *Z. Astrophys.*, **49**, 131.
Jakobsson, L. R., 1967. *Ark. Fys.*, **34**, 19.
Johansson, L., 1966. *Ark. Fys.*, **31**, 201.
Karstenson, F., 1965. *Z. Phys.*, **187**, 165.
Lambert, D. L., 1967a. *Mon. Not. R. astr. Soc.*, **138**, 143.
Lambert, D. L., 1967b. To be published.
Lambert, D. L. & Swings, J. P., 1967. In preparation.
Martin, W. C., 1959. *J. opt. Soc. Am.*, **49**, 1071.
Miessner, K. W., Bartelt, O. & Eckstein, L., 1933. *Z. Phys.*, **86**, 54.
Mohler, O. C., 1955. *A Table of Solar Spectrum Wavelengths* 11 984–25 578 Å, University of Michigan Press, Ann Arbor.
Moore, C. E., 1945. *A Multiplet Table of Astrophysical Interest*, National Bureau of Standards, Washington.
Moore, C. E., 1949. *Atomic Energy Levels*, Vol. 1., National Bureau of Standards, Washington.
Moore, C. E., Minnaert, M. G. J. & Houtgast, J., 1966. *The Solar Spectrum* 2935–8770 Å, National Bureau of Standards, Washington.
Mugglestone, D. & O'Mara, B. J., 1966. *Mon. Not. R. astr. Soc.*, **132**, 87.
Müller, E. A., 1967. Report of Symposium No. 1. Ass. Int. Geochem. Cosmochem, Paris. In press.
Ostrovskii Yu. I. & Penkin, N. P., 1962. *Optics Spectrosc.*, **12**, 379.
Righini, G., 1935. *Z. Astrophys.*, **10**, 344.
Risberg, P., 1956. *Ark. Fys.*, **10**, 583.
Stephenson, G., 1951. *Proc. phys. Soc.*, A**64**, 458.
Stewart, J. C. & Rotenberg, M., 1965. *Phys. Rev.*, **140**A, 1508.
Swensson, J. W., 1966. *Z. Astrophys.*, **64**, 11.
Toresson, Y. G., 1960. *Ark. Fys.*, **18**, 417.
Utrecht Observatory Staff, 1960. *Rech. astr. Obs. Utrecht*, **15**.
Vardya, M. S., 1966. Observatory, **86**, 30.
Waddell, J. H., 1962. *Astrophys. J.*, **136**, 223.
Warner, B., 1967. To be published.